Adduct formation of [(η^7-C$_7$H$_7$)Hf(η^5-C$_5$H$_5$)] with isocyanides, phosphines and N-heterocyclic carbenes: An experimental and theoretical study

Susanne Büschel, Thomas Bannenberg, Cristian G. Hrib, Andreas Glöckner, Peter G. Jones, Matthias Tamm *

Institut für Anorganische und Analytische Chemie, Technische Universität Braunschweig, Hagenring 30, D-38106 Braunschweig, Germany

ABSTRACT

The reactions of [(η^7-C$_7$H$_7$)Hf(η^5-C$_5$H$_5$)] (**1b**) with the two-electron donor ligands *tert*-butyl isocyanide (*t*BuNC), 2,6-dimethylphenyl isocyanide (XyNC), 1,3,4,5-tetramethylimidazolin-2-ylidene (IMe) and trimethylphosphine (PMe$_3$) are reported. The 1:1 complexes [(η^7-C$_7$H$_7$)Hf(η^5-C$_5$H$_5$)L] (**2b**, L = *t*BuNC; **3b**, L = XyNC; **4b**, L = IMe, **5b**, L = PMe$_3$) have been isolated in crystalline form, and their molecular structures have been determined by X-ray diffraction analyses. The stabilities of these hafnium complexes were probed via spectroscopic and theoretical methods, and the results were compared to those previously reported for the corresponding zirconium complexes derived from [(η^7-C$_7$H$_7$)Zr(η^5-C$_5$H$_5$)] (**1a**). The X-ray crystal structure of the PMe$_3$ adduct [(η^7-C$_7$H$_7$)Zr(η^5-C$_5$H$_5$)(PMe$_3$)] (**5a**) was also established.

© 2009 Elsevier B.V. All rights reserved.

1. Introduction

Sandwich complexes, in which a metal atom is located between the faces of two parallel and planar aromatic ring structures, represent the most prominent class of organometallic compounds, and the discovery, synthesis and structural elucidation of the first and still most famous representatives, bis(η^5-cyclopentadienyl)iron (ferrocene) [1] and bis(η^6-benzene)chromium [2], in the early 1950s mark the beginning of modern organometallic chemistry. This area continues to be dominated by transition metal complexes containing η^5-cyclopentadienyl (Cp) and η^6-arene ligands, whereas comparatively little use has been made of cycloheptatrienyl (Cht) ligands, although early-transition metal Cht–Cp metal complexes of the type [(η^7-C$_7$H$_7$)M(η^5-C$_5$H$_5$)] (M = group 4–6 metal) have been known for more than three decades [3]. The interest in these complexes has become revitalized by independent reports from the groups of Elschenbroich, Braunschweig and Tamm on the preparation of *ansa*-Cht–Cp complexes such as those shown in Fig. 1, which have been obtained from the 16-, 17- and 18-electron sandwich complexes containing titanium, vanadium and chromium, respectively [4–7]. For M = Ti, we were able to demonstrate that the introduction of a silylene bridge makes the coordinating rings significantly non-parallel and opens a potential vacancy at the titanium centre; thus adducts with carbon monoxide and isocyanides have been observed [5a], whereas the parent 16-electron complex [(η^7-C$_7$H$_7$)Ti(η^5-C$_5$H$_5$)] (troticene) does not form adducts with simple two-electron ligands. In contrast, the corresponding zirconium complex [(η^7-C$_7$H$_7$)Zr(η^5-C$_5$H$_5$)] (trozircene, **1a**) has been shown to react with isocyanides [8], phosphines and N-heterocyclic carbenes [9] without the need to resort to the introduction of a bridging unit (Scheme 1).

These reactivity studies also revealed that trozircene has only a limited propensity to interact efficiently with σ-donor/π-acceptor ligands; it does not act like a complex containing zirconium in a lower oxidation state but rather bears a closer resemblance to more Lewis acidic Zr(IV) complexes. Based on theoretical calculations [4,10], this behaviour can be mainly attributed to the strong and appreciably covalent metal–cycloheptatrienyl interaction leading to highly stabilized frontier orbitals and consequently to a diminishing π-electron release capability, which is also consistent with the assumption of a charge of -3 rather than +1 on the cycloheptatrienyl ligand in this Cht–Cp metal complex. Surprisingly, the preparation and molecular structure of the analogous hafnium complex [(η^7-C$_7$H$_7$)Hf(η^5-C$_5$H$_5$)] (trohafcene, **1b**) have not yet been reported, and consequently, no reactivity studies are available for this sandwich complex; these issues are addressed by the publication at hand. It should be noted that the Cp* analogue [(η^7-C$_7$H$_7$)Hf(η^5-C$_5$Me$_5$)] is known [11] and that the formation of thermally labile phosphine adducts has been described for the related indenyl complex [(η^7-C$_7$H$_7$)Hf(η^5-C$_9$H$_7$)] [12].

* Corresponding author. Tel.: +49 (0) 531 391 5309; fax: +49 (0) 531 391 5387.
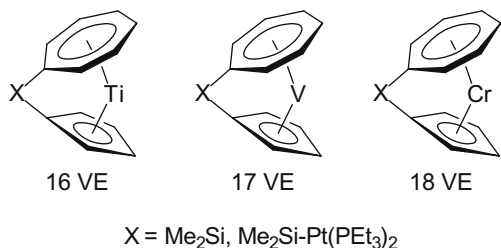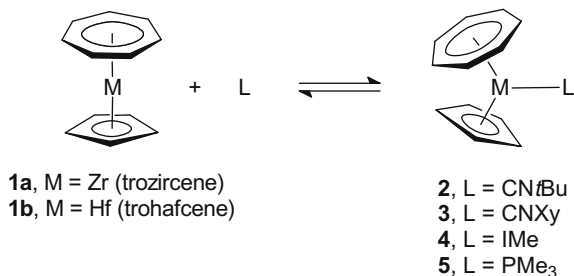*E-mail address:* m.tamm@tu-bs.de (M. Tamm).

Fig. 1. *ansa*-Cycloheptatrienyl–cyclopentadienyl transition metal complexes.

Scheme 1. Formation of trozircene and trohafcene complexes.

2. Experimental

2.1. General information

All operations were performed in a glove box under a dry argon atmosphere (MBraun 200B) or on a high vacuum line using Schlenk techniques. All solvents were purified by a solvent purification system from MBraun GmbH and stored over molecular sieve (4 Å) prior to use. The ^1H, ^{13}C, and ^{31}P-NMR spectra were recorded on Bruker DPX 200, Bruker AV 300, and Bruker DRX 400 devices. The chemical shifts are expressed in parts per million (ppm) and are referenced to residual ^1H or ^{13}C resonances of the solvent or to external H_3PO_4. Coupling constants (J) are reported in Hertz (Hz), and splitting patterns are indicated as s (singlet), d (doublet), t (triplet), m (multiplet) and br (broad). Elemental analysis (C, H, N) was performed by combustion and gas chromatographical analysis with an Elementar varioMICRO. The starting materials *tert*-butyl isocyanide (*t*BuNC), 2,6-dimethylphenyl isocyanide (XyNC) and trimethylphosphine (PMe$_3$) were obtained from Sigma–Aldrich and used without further purification. Cycloheptatriene (C_7H_8) was distilled prior to use. 1,3,4,5-Tetramethylimidazolin-2-ylidene (IMe) [13] and [(η^5-C_5H_5)$_2$HfCl$_2$] [14] were synthesized according to literature methods. The preparation and characterization of the zirconium complexes **2a**, **3a** [8], **4a** and **5a** [9] were reported elsewhere.

2.2. Preparation of [(η^7-C_7H_7)Hf(η^5-C_5H_5)] (**1b**)

Hafnocene dichloride (2.04 g, 5.38 mmol) was dissolved in THF (12 mL) and added to a Schlenk flask containing 3 eq. magnesium (0.39 g, 16 mmol), a catalytic amount of anhydrous FeCl$_3$ (2.1 mg) and C_7H_8 (1.12 mL, 10.8 mmol) in THF (4 mL), resulting in a green mixture. At 60 °C, the mixture was stirred for 24 h, whereupon the colour changed from brown to brownish-black. The solids were removed by filtration, and the solvent was evaporated. The excess of cycloheptatriene was removed by heating at 80 °C under high vacuum for 2.5 h. Sublimation at 170 °C afforded an orange-red solid. Yield: 0.48 g (1.4 mmol, 27 %). Single-crystals were grown by diffusion of *n*-hexane into a saturated solution of **1b** in THF. Anal. Calc.

for C$_{12}$H$_{12}$Hf (334.7): C, 43.06; H, 3.61. Found: C, 43.17; H, 3.64%. ^1H NMR (300 MHz, C_6D_6, 25 °C): δ 5.15 (s, 5H, C_5H_5), 5.10 (s, 7H, C_7H_7). ^{13}C NMR (75 MHz, C_6D_6, 25 °C): δ 98.5 (C_5H_5), 76.3 (C_7H_7).

2.3. Preparation of [**1b**(CN*t*Bu)] (**2b**)

Two hundred and two milligrams (0.60 mmol) of **1b** were dissolved in 12 mL of toluene and 0.06 mL (0.6 mmol) of *tert*-butyl isocyanide (*t*BuNC) were added to give an orange-yellow solution. The mixture was stirred for 10 min, and the solvent was evaporated. The bright yellow solid was washed with hexane and dried *in vacuo* to give 201 mg (0.48 mmol, 80%) of **2b**. Anal. Calc. for C$_{17}$H$_{21}$NHf (417.9): C, 48.87; H, 5.07; N, 3.35. Found: C, 48.24; H, 5.06; N, 3.37%. ^1H NMR (300 MHz, C_7D_8, 25 °C): δ 5.28 (s, 5H, C_5H_5), 4.63 (s, 7H, C_7H_7), 0.74 (br, 9H, CCH_3). ^{13}C NMR (75 MHz, C_7D_8, 25 °C): δ 150.7 (*C*NR), 96.1 (C_5H_5), 78.5 (C_7H_7), 55.4 (*C*CH$_3$), 29.1 (CCH_3). IR (ATR): 2148 cm^{-1} (ν(C≡N)).

2.4. Preparation of [**1b**(CNXy)] (**3b**)

To a solution of 170 mg (0.51 mmol) of **1b** in 15 mL of toluene was added 67 mg (0.51 mmol) of dimethylphenylisocyanide (XyNC) in 5 mL toluene. The solution turned red immediately, and a red solid formed. The mixture was stirred for 15 min at ambient temperature, and the solvent was removed under reduced pressure. The red solid was washed with hexane and dried *in vacuo* to give 204 mg (0.44 mmol, 86%) of a bright red solid. Suitable crystals for X-ray diffraction analysis were grown by diffusion of hexane into a saturated THF solution of **3b**. Anal. Calc. for C$_{21}$H$_{21}$NHf (465.9): C, 54.14; H, 4.54; N, 3.01. Found: C, 53.98; H, 4.72; N, 3.10%. ^1H NMR (300 MHz, THF-d_8, 25 °C): δ 7.14 (m, 2H, C_6H_3), 7.11 (m, 1H, C_6H_3), 5.39 (s, 5H, C_5H_5), 4.43 (s. 7H, C_7H_7), 2.40 (s, 6H, CCH_3). ^{13}C NMR (75 MHz, THF-d_8, 25 °C): δ 135.3 (*i*-C_3H_6), 128.9 (C_3H_6), 128.3 (C_3H_6), 128.0 (C_3H_6), 96.2 (C_5H_5), 78.8 (C_7H_7), 18.2 (CCH_3). IR (Nujol): 2129 cm^{-1} (ν(C≡N)).

2.5. Preparation of [**1b**(IMe)] (**4b**)

Forty-five milligrams (0.37 mmol) of 1,3,4,5-tetramethylimidazolin-2-ylidene (IMe) were dissolved in THF (5 mL) and added dropwise to a solution of **1b** (122 mg, 0.37 mmol) in THF (10 mL) at room temperature. An immediate colour change from red to yellow was observed. After 30 min, the solvent was removed *in vacuo*. The yellow residue was washed with a small amount of hexane and dried *in vacuo* to give 123 mg (0.27 mmol, 74%) of the desired compound **4b**. Anal. Calc. for C$_{19}$H$_{21}$N$_2$Hf (455.9): C, 50.06; H, 4.64; N, 6.14. Found: C, 50.24; H, 5.31; N, 6.16%. ^1H NMR (300 MHz, C_6D_6, 25 °C): δ 5.20 (s, 5H, C_5H_5), 4.63 (s, 7H, C_7H_7), 3.30 (s, 6H, (N-CH_3)$_2$), 1.34 (s, 6H, (C-CH_3)$_2$). ^{13}C NMR (75 MHz, C_6D_6, 25 °C): δ 192.6 (Hf-*C*), 122.9 ((*C*-CH$_3$)$_2$), 96.2 (C_5H_5), 77.4 (C_7H_7), 36.1 ((N-CH_3)$_2$), 8.4 ((C-CH_3)$_2$).

2.6. Preparation of [**1b**(PMe$_3$)] (**5b**)

1b (56 mg, 0.17 mmol) was dissolved in toluene (6 mL) at room temperature. An equimolar amount of PMe$_3$ (0.0017 mL, 0.17 mmol) was added and an immediate colour change to yellow was observed. The solution was stirred at ambient temperature for 5 min. Yellow crystals of compound **5b** were obtained by cooling a solution of 50.2 mg (0.15 mmol) in 12 mL of toluene with an excess of PMe$_3$ (0.03 mL, 0.3 mmol) to −35 °C. ^1H NMR (200 MHz, C_7D_8, 25 °C): δ 5.08 (s, 5H, C_5H_5), 4.58 (s, 7H, C_7H_7), 0.66 (d, 9H, $^2J_{PH}$ = 3.54 Hz, PMe$_3$). ^{13}C NMR (50 MHz, C_7D_8, 25 °C): δ 96.3 (C_5H_5), 76.6 (C_7H_7), 17.9 ($^1J_{PC}$ = 7.12 Hz, PMe$_3$). ^{31}P{^1H} NMR (81 MHz, C_7D_8, 25 °C): δ −50.3 (s, *P*Me$_3$). Attempts to isolate this

species in pure form were hampered by the lability of the coordinated phosphine ligand.

2.7. Theoretical calculations

The calculations were performed using the GAUSSIAN03 package [15]. All structures were fully optimized on the density functional theory (DFT) level employing the B3LYP or the M05-2X hybrid functional [16,17]. For all main-group elements (C, H, N and P) the all-electron triple-ζ basis set (6-311G**) was used, whereas for the group 4 transition metals Zr and Hf a small-core relativistic ECP together with the corresponding triple-ζ valence basis set was employed (Stuttgart RSC 1997 ECP) [18]. The standard enthalpies for the formation of trozircene and trohafcene complexes were calculated by subtracting the enthalpies of the ground-state electronic structures of **1a** and **1b** and the respective ligand from those of the resulting complexes.

2.8. Single-crystal X-ray structure determinations

Crystal data and numerical details of the structure determinations are presented in Table 1. Data were recorded at low temperature on various area detectors (Bruker, Oxford Diffraction) using Mo Kα radiation and corrected for absorption using the multi-scan method. Structures were refined with SHELXL-97 [19]. Hydrogen atoms were included using a riding model or rigid methyl groups. Special features of refinement: The methyl hydrogens at C8 are disordered about the mirror plane. Compound **3b** is pseudosymmetric, whereby the isonitrile ligand occupies what would be a mirror plane in $P2_1/m$. This pseudosymmetry is the probable cause of the distorted ellipsoids of the other ring carbons. The structure was refined as an enantiomeric twin.

3. Results and discussion

3.1. Synthesis and structural characterization of [(η^7-C$_7$H$_7$)Hf(η^5-C$_5$H$_5$)](1b)

Trohafcene (**1b**) was prepared in moderate yield by reduction of [(η^5-C$_5$H$_5$)$_2$HfCl$_2$] with magnesium in the presence of an excess of cycloheptatriene, C$_7$H$_8$. After sublimation, **1b** was isolated as an orange crystalline solid. As expected, the C$_7$H$_7$ and C$_5$H$_5$ rings give
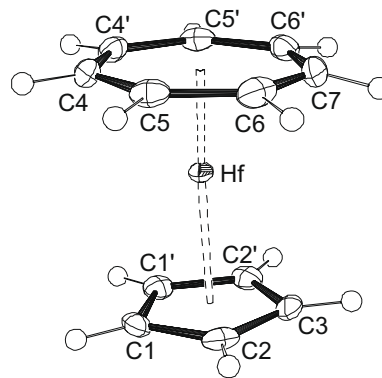

Fig. 2. Molecular structure of trohafcene (**1b**).

rise to only two resonances in the ^{1}H NMR and ^{13}C NMR spectra. All resonances (in C$_6$D$_6$) are observed at slightly higher field than those reported for trozircene (**1a**) [8]. Similarly to **1a**, the chemical shifts for the Cht and Cp hydrogen atoms (5.10 and 5.15 ppm) are almost identical, whereas the ^{13}C NMR resonance of the C$_7$H$_7$ ring is observed at a significantly higher field (76.3 ppm) than that of the C$_5$H$_5$ ring (98.5 ppm).

Since the Cp* analogue [(η^7-C$_7$H$_7$)Hf(η^5-C$_5$Me$_5$)] constitutes the only structurally characterized Cht–Cp hafnium sandwich complex to date [11c], the molecular structure of **1b** was determined by X-ray diffraction analysis (Fig. 2). **1b** is isostructural with its titanium and zirconium congeners [8,20] and crystallizes in the space group *Pnma*. The hafnium atom and one carbon atom in each ring reside on a crystallographic mirror plane. As these two carbon atoms, C3 and C7, adopt a *cis* orientation, the conformation of the two rings can be regarded as being eclipsed. This situation is opposite to the staggered conformation found in the Cp* analogue, which otherwise exhibits very similar structural parameters [11c]. Both hydrocarbon rings are virtually planar, and the centroid–metal–centroid angle (176.6°) is close to linearity. Selected bond lengths and angles are summarized in Table 1; in agreement with the trend of the metal radii [21], the metal–carbon distances in **1b** are shorter than those reported for **1a** [8]. As expected, the metal–carbon bonds to the seven-membered ring are significantly shorter than those to the five-membered ring, revealing a much stronger interaction between the metal centre and the cycloheptatrienyl ring [4].

Table 1
Crystallographic data for complexes **1b**, **3b**, **4b**, **5a** and **5b**.

	1b	3b	4b	5a	5b
Empirical formula	C$_{12}$H$_{12}$Hf	C$_{21}$H$_{21}$HfN	C$_{19}$H$_{24}$HfN$_2$	C$_{15}$H$_{21}$PZr	C$_{15}$H$_{21}$HfP
Formula weight	334.71	465.88	458.89	323.51	410.78
T (°C)	−140	−140	−140	−173	−173
λ (Å)	0.71073	0.71073	0.71073	0.71073	0.71073
Crystal system	Orthorhombic	Monoclinic	Monoclinic	Orthorhombic	Orthorhombic
Space group	*Pnma*	*P*2(1)	*P*2(1)/*n*	*Pnma*	*Pnma*
a (Å)	11.0557(10)	10.8155(12)	10.8065(5)	9.6542(6)	9.6113(3)
b (Å)	10.5825(10)	6.8027(8)	13.7863(6)	10.7216(6)	10.7458(3)
c (Å)	8.1493(8)	11.5390(12)	11.5686(5)	13.2254(6)	13.1268(3)
α (°)	90	90	90	90	90
β (°)	90	101.579(3)	106.4240(10)	90	90
γ (°)	90	90	90	90	90
V (Å^3)	953.44(16)	831.70(16)	1653.18(13)	1368.94(13)	1355.75(6)
Z	4	2	4	4	4
Crystal size (mm^3)	0.23 × 0.21 × 0.17	0.38 × 0.36 × 0.32	0.22 × 0.21 × 0.19	0.38 × 0.27 × 0.26	0.33 × 0.18 × 0.14
Completeness to theta (%)	99.8	99.6	100.0	98.7	96.9
Reflections collected	19640	18289	35402	35141	42047
$R_{(int)}$	0.0241	0.0186	0.0233	0.0195	0.0276
$R_1 (I > 2\sigma(I))$	0.0127	0.0134	0.0138	0.0193	0.0126
wR_2	0.0351	0.0345	0.0354	0.0521	0.0279
$\Delta\rho$ (e Å^{-3})	0.484/−1.254	0.896/−0.891	1.077/−0.388	0.638/−0.551	1.108/−0.797
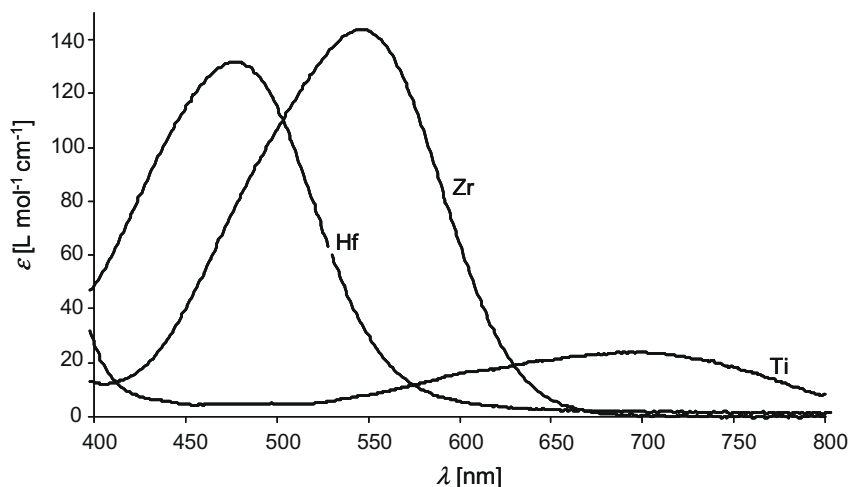
Fig. 3. UV/vis spectra of $[(\eta^7\text{-}C_7H_7)M(\eta^5\text{-}C_5H_5)]$ (M = Ti, Zr, Hf).

The colours of the group 4 sandwich complexes $[(\eta^7\text{-}C_7H_7)M(\eta^5\text{-}C_5H_5)]$ are blue (M = Ti), purple (M = Zr, **1a**) and orange-red (M = Hf, **1b**), indicating that the absorption maximum in the visible spectrum is shifted to higher energy (blue-shifted) upon going from Ti to Zr and Hf. A hypsochromic trend is confirmed by UV/vis spectroscopic characterization of the three sandwich complexes (Fig. 3), and the visible band (in toluene) is shifted from λ = 693 nm (M = Ti, ε = 24 L mol^{-1} cm^{-1}) to 546 nm (M = Zr, ε = 144 L mol^{-1} cm^{-1}) and 477 nm (M = Hf, ε = 132 L mol^{-1} cm^{-1}). The simplest interpretation is to assign these absorptions to a one-electron HOMO–LUMO excitation, which can be regarded as being partly a d–d transition and partly a ligand-to-metal charge transfer (LMCT) [22], since significant mixing of metal and Cht ligand orbital character has experimentally [23] and theoretically [4,10] been deduced for the highest occupied molecular orbitals (HOMOs) in these Cht–Cp complexes. In addition, the calculated HOMO–LUMO gap in $[(\eta^7\text{-}C_7H_7)M(\eta^5\text{-}C_5H_5)]$ increases in the order Ti < Zr < Hf [4], consistent with the observed blue-shifting of the optical absorption bands (Fig. 3). The greater intensity of the absorptions observed for the Zr and Hf complexes **1a** and **1b** in comparison with their Ti congener can be explained by relaxation of the Laporte selection rule for 4d and 5d transition metals [24]. It should also be noted that similar trends have been reported for the UV/vis spectra of the Cp* complexes $[(\eta^7\text{-}C_7H_7)M(\eta^5\text{-}C_5Me_5)]$ (M = Ti, Zr, Hf) [11a,25].

3.2. Reactivity of $[(\eta^7\text{-}C_7H_7)Hf(\eta^5\text{-}C_5H_5)]$(**1b**) towards σ-donor/π-acceptor ligands

The addition of *tert*-butyl isocyanide (*t*BuNC) or 2,6-dimethylphenyl isocyanide (XyNC) to a solution of **1b** in toluene afforded the isocyanide complexes **2b** and **3b** in high yield as bright yellow (for *t*BuNC) or bright red (for XyNC) crystalline solids (Scheme 1). Upon coordination of the isocyanides, the NMR signals of the Cht protons in **2b** and **3b** are both shifted upfield, while the signals of the Cp protons are shifted downfield. The opposite trend is observed in the ^{13}C NMR spectra of **2b** and **3b**; however, the resonances are only marginally shifted in comparison with those of **1b**. In a similar fashion to that described for the corresponding trozircene complex **2a** [8], NMR measurements on samples containing **1b** and substoichiometric amounts of *t*BuNC showed only one set of NMR signals for the C_7H_7 and C_5H_5 ring protons, indicating fast ligand exchange on the NMR time scale at room temperature. For a 3:2 mixture, a variable-temperature ^1H NMR study showed significant broadening at room temperature and coalescence of the sig-

nals in a temperature range between -10 and $-20\,^\circ C$, slightly higher than the coalescence temperature reported for **2a** [8]. Below $-40\,^\circ C$, separate and clearly resolved resonances are observed for **1b** and **2b**.

In the IR spectra, the CN stretching vibrations are at 2148 cm^{-1} (**2b**) and 2129 cm^{-1} (**3b**), which is only slightly shifted with respect to the values for the free, uncoordinated isocyanides [26]. These observations indicate that metal-to-ligand π back-bonding is weak, albeit slightly more pronounced than in the corresponding trozircene complexes **2a** and **3a** [8]. These wavenumbers are nevertheless significantly smaller than those reported for d^0-configured cationic hafnium(IV) complexes [27], e.g. ν(CN) = 2211 cm^{-1} in $[Cp_3Hf(CN\text{t}Bu)]^+$ [27a]. Higher values have also been reported for the mixed carbonyl–isocyanide hafnium(II) complex $[Cp_2Hf(CO)(CN\text{t}Bu)]$ (ν_{CO} = 1810 cm^{-1}, ν_{CN} = 2192 cm^{-1}) [28] and for the *t*BuNC adduct of the structurally related cyclooctatetraenyl complex $[(\eta^8\text{-}C_8H_8)Hf(\eta^4\text{-}C_8H_8)]$ (ν_{CN} = 2177 cm^{-1}) [29]. Only for $[Cp^*_2HfCl(i\text{Pr-DAB})(CNXy)]$, which contains an electron-rich enediamide ligand derived from 1,4-diisopropyl-1,4-diaza-1,3-butadiene, was a smaller wavenumber (2070 cm^{-1}) reported [30].

Single-crystals of both complexes were obtained by slow diffusion of hexane into THF solutions of **2b** and **3b** and were subjected to X-ray diffraction analyses. Whereas **2b** displayed an unresolvable disorder of the cycloheptatrienyl ring (possibly by free rotation about the metal-ring axis, or by multiple static positions thus generated), the molecular structure of **3b** could be satisfactorily refined despite pseudosymmetry (Fig. 4). Coordination of the XyNC ligand leads to a marked deviation from the coplanar orientation of the Cp and Cht rings that is observed for **1b**; the angle
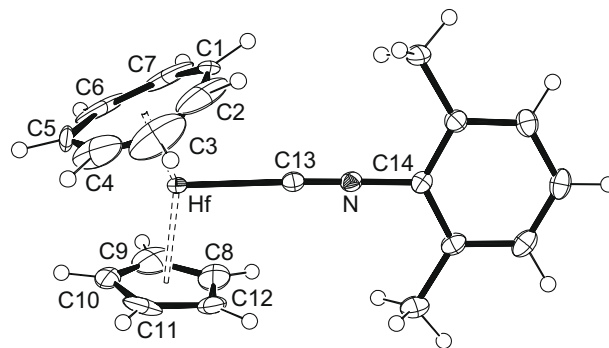

Fig. 4. Molecular structure of **3b**.

Table 2
Selected bond lengths (Å) and angles (°) in complexes **1b**, **3b**, **4b**, **5a** and **5b**.

	1b	3b	4b	5b	5a
M–L	–	2.306(2)	2.394(2)	2.7851(5)	2.8307(5)
M–C$_{Cht}$	2.296(3)–2.307(2)	2.317(4)–2.419(2)	2.335(2)–2.451(2)	2.328(2)–2.454(2)	2.3567(13)–2.468(2)
M–C$_{Cp}$	2.458(2)– 2.471(2)	2.486(3)–2.492(3)	2.503(2)–2.524(2)	2.498(2)–2.5168(14)	2.529(2)–2.5439(11)
M–Ct7[a]	1.614	1.730	1.744	1.737	1.764
M–Ct5[b]	2.151	2.184	2.209	2.203	2.235
Ct5–M–Ct7	176.6	151.3	147.5	146.5	146.9
L–M–Ct5	–	98.7	98.6	102.6	102.4
L–M–Ct7	–	109.8	113.9	110.9	110.4

[a] Ct7 = centroid of the Cht ring.
[b] Ct5 = centroid of the Cp ring.

subtended at the metal centre by the ring centroids is 151.3°. In addition, coordination also results in a pronounced elongation of the metal–carbon bonds (Table 2), in particular of those to the seven-membered ring. As expected from a theoretical study of the binding in the zirconium analogue **3a** [8], the 2,6-dimethylphenyl isocyanide ligand in **3b** adopts a vertical conformation with a coplanar orientation toward the non-crystallographic mirror plane including the Hf atom and the centroids of the Cht and Cp rings. This orientation is favourable, since it allows the alignment of the LUMO of the isocyanide ligand with the HOMO of the Cht–Hf–Cp complex fragment for optimum π interaction. The Hf–CN bond distance of 2.306(2) Å is slightly longer than was reported for the only other structurally characterized hafnium–isocyanide complex [Cp₃Hf(CN*t*Bu)][B(CH₃)(C₆F₅)₃] (2.275(4) Å) [31]. The Hf–C–N–C moiety is nearly linear (Hf–C13–N = 178.2(2)° C13–N–C14 = 177.8(6)°), and the C13–N distance is 1.154(3) Å, which is almost identical with the C–N distance in the free unccordinated isocyanide (1.160(3) Å) [32].

The addition of 1,3,4,5-tetramethylimidazolin-2-ylidene (IMe) to a solution of **1b** in THF gave rise to a colour change from orange-red to bright yellow, and the carbene adduct **4b** could be isolated in good yield (Scheme 1). In a similar fashion to that described for the isocyanide complexes **2b** and **3b**, the C₇H₇ ¹H NMR resonances are shifted upfield with respect to trohafcene (**1b**), whilst the resonances associated with the C₅H₅ ring are shifted downfield; this trend is again reversed in the ¹³C NMR spectrum. The resonance assigned to the carbene carbon atom is shifted to higher field (192.6 ppm) compared to the free carbene (212.6 ppm). Single-crystals of **4b** could be grown from THF/hexane solution, and its molecular structure is shown in Fig. 5; pertinent data are recorded in Table 2. In comparison to **1b**, carbene coordination results in a significant lengthening of the Hf-C bonds to the cycloheptatrienyl and to a lesser extent to the cyclopentadienyl rings; this trend is more pronounced than observed for the isocyanide complex **3b**, and the angle subtended at the metal cen-

tre by the ring centroids is narrower (147.5°). The horizontal conformation of the carbene ligand is similar to that observed for the corresponding zirconium complex **4a** [9], suggesting that the N-heterocyclic carbene is acting as a pure σ-donor ligand. The Hf–C13 bond length is 2.394(2) Å and falls in the same range reported for the Hf–C(carbene) distances in the complexes *trans*-[(I*i*Pr)₂HfCl₄] (2.401(2) Å) and [(I*i*Pr)HfCl₅]⁻ (2.406(6) Å) [33,34].

Treatment of trohafcene (**1b**) with equimolar amounts of PMe₃ also afforded a colour change from orange-red to yellow (Scheme 1), and interaction with the phosphine ligand is indicated by similar effects on the C₇H₇ and C₅H₅ resonance signals as those described for the ¹H and ¹³C NMR spectra of **2b**, **3b** and **4b** (vide supra). The ³¹P{¹H} NMR spectrum of **5b** displays a signal at −50.3 ppm, which is upfield from the resonance of free PMe₃ (−60.1 ppm) and similar to the chemical shift reported for the Zr analogue **5a** (−52.2 ppm) [9]. As previously described for **5a**, isolation of pure **5b** was hampered by its lability, since exposure of solutions and also of crystalline material to vacuum results in loss of coordinated PMe₃ and re-isolation of **1b**. This is a common observation for other PMe₃ adducts of group 4 metals [35]. Nevertheless, single-crystals of **5b** could be obtained from a solution containing **1b** and an excess of PMe₃ at −35 °C and were subjected to an X-ray diffraction analysis. In a similar fashion, the molecular structure of **5a**, which had previously resisted isolation in pure form, could also be established. Fig. 6 shows the molecular structure of **5b**, and selected bond lengths and angles of both **5a** and **5b** are assembled in Table 2. **5a** and **5b** are isostructural and crystallize in the orthorhombic space group *Pnma* with each molecule residing on a crystallographic mirror plane. In agreement with the trend of the metal radii [21], all metal-element bond lengths in the hafnium complex **5b** are shorter than those in **5a**. The metal–phosphorus distances are 2.8307(5) Å (in **5a**) and 2.7851(5) Å (in **5b**), which are at the top end of the range that has been previously established for zirconium and hafnium PMe₃ complexes [36]. The
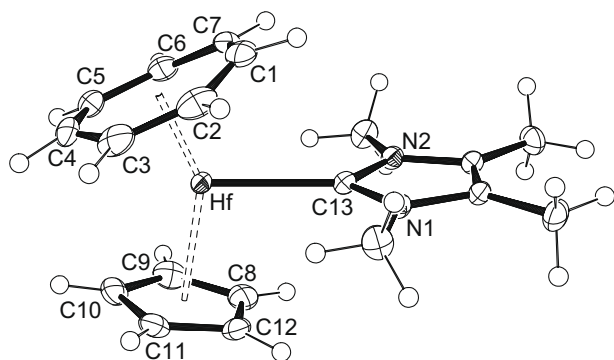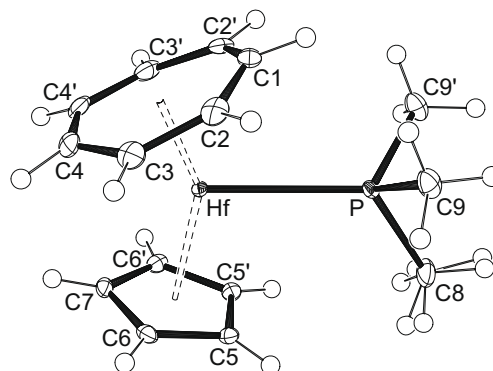

Fig. 5. Molecular structure of **4b**.

Fig. 6. Molecular structure of **5b**, the hydrogen atoms at C8 are disordered over two positions.

Table 3
Standard enthalpies for the formation of selected trozircene and trohafcene complexes; calculated and experimental metal–ligand distances.

Complex (M)	L	ΔH°_{calcd} (kJ mol^{-1})		d(M–L)$_{calcd}$ (Å)		d(M–L)$_{exp}$ (Å)
		B3LYP	M05-2X	B3LYP	M05-2X	
2a (Zr)	tBuNC	−36.5	−45.4	2.38	2.42	2.376(3)
2b (Hf)	tBuNC	−43.3	−51.2	2.36	2.38	2.35[a]
3a (Zr)	XyNC	−38.2	−49.5	2.36	2.40	2.367(2)[b]
3b (Hf)	XyNC	−46.0	−45.5	2.32	2.36	2.306(2)
4a (Zr)	IMe	−56.3	−97.3	2.51	2.48	2.445(2)
4b (Hf)	IMe	−63.1	−99.0	2.47	2.45	2.394(2)
5a (Zr)	PMe$_3$	−2.3	−43.1	2.94	2.87	2.8307(5)
5b (Hf)	PMe$_3$	−3.5	−45.7	2.90	2.84	2.7851(5)

[a] Disordered structure with two independent molecules in the asymmetric unit.
[b] Unpublished results (with R.D. Ernst and A.M. Arif).

only other structurally characterized complexes containing both cycloheptatrienyl and phosphine ligands, *viz.* [(η^7-C$_7$H$_7$)Zr(PMe$_3$)$_2$I] and the dmpe-adduct of the indenyl complex [(η^7-C$_7$H$_7$)Hf(η^5-C$_9$H$_7$)], feature very similar Zr–P and Hf–P distances of 2.811(1) and 2.788(7) Å, respectively [12a,37].

3.3. Theoretical studies on **1** and **2**

The structures of all complexes **1**–**5** have been optimized with DFT methods employing the B3LYP and M05-2X hybrid functional. Presentations of all calculated structures together with Cartesian coordinates of their atomic positions are provided in the Supporting information. In general, the calculated geometries are in good agreement with those determined by X-ray diffraction analyses, and the experimentally observed orientations of the isocyanide, carbene and phosphine ligands have satisfactorily been reproduced. Table 3 summarizes the calculated and experimental metal–ligand bond lengths together with the calculated enthalpies of formation for the trozircene and trohafcene adducts **2**–**5**. The B3LYP values suggest that the formation of each hafnium complex is more exothermic than the formation of the corresponding zirconium complex. As expected, the carbene complexes **4** are considered to be thermodynamically more stable than the isocyanide complexes **2** and **3**, which is probably a result of the strong σ-donating ability of the IMe ligand [38]. In contrast, the formation of the phosphine adducts **5** is calculated to be almost thermoneutral, which seems to be in accord with the lability of these complexes in solution. It should be noted, however, that the computed metal–P distances are significantly longer than those observed by X-ray diffraction and that the deviation between the theoretical and experimental values is considerably more pronounced than in the case of the isocyanide and carbene complexes **2**–**4**.

Since it has been demonstrated that B3LYP is unable properly to describe medium-range dispersion interactions [39], which might also significantly contribute to the overall binding energy in the phosphine complexes **5** [40], the M05-2X functional developed by Truhlar for better consideration of non-covalent interactions was additionally applied [39b]. This results in an appreciably stronger stabilization of **5a** and **5b** by more than 40 kJ mol^{-1} in comparison with the B3LYP results and also yields a better correlation between the calculated and experimental metal–P distances. The carbene complexes **4** are also additionally stabilized by the same order of magnitude upon applying the M05-2X functional, which is in line with the greater electron-donating properties of N-heterocyclic carbene ligands compared to tertiary phosphines [41,42]. In contrast, the differences in the enthalpies of the isocyanide complexes **2** and **3** are significantly less pronounced, suggesting that non-covalent interactions are less important for the overall binding of slender isocyanides with more remote substitu-

ents. Further studies, *inter alia* by means of NMR titration techniques [8] or thermochemical methods [42,43] will be carried out to experimentally quantify and confirm the different stabilities of the Zr and Hf Cht–Cp complexes, since subtle differences in the reactivities of related zirconocene and hafnocene complexes have recently led to the isolation of remarkable organohafnium complexes and to "hafnium's foray into the limelight" [44,45].

Acknowledgement

Appendix A. Supplementary data

CCDC 713615, 713616, 713617, 713618 and 713619 contain the supplementary crystallographic data for compounds **2b**–**5b** and **5a**. These data can be obtained free of charge from The Cambridge Crystallographic Data Centre via www.ccdc.cam.ac.uk/data_request/cif. Supplementary data associated with this article can be found, in the online version, at doi:10.1016/j.jorganchem.2009.01.055.

References

[1] (a) Special issue: 50th anniversary of the discovery of ferrocene; R.D. Adams (Ed.), J. Organomet. Chem. 637–639 (2001) 1.;
(b) P. Laszlo, R. Hoffmann, Angew. Chem., Int. Ed. 39 (2000) 123;
(c) H. Werner, Angew. Chem., Int. Ed. 16 (1977) 1.
[2] (a) D. Seyferth, Organometallics 21 (2002) 1520;
(b) D. Seyferth, Organometallics 21 (2002) 2800.
[3] M.L.H. Green, D.K.P. Ng, Chem. Rev. 95 (1995) 439.
[4] M. Tamm, Chem. Commun. (2008) 3089.
[5] (a) M. Tamm, A. Kunst, T. Bannenberg, E. Herdtweck, P. Sirsch, C.J. Elsevier, J.M. Ernsting, Angew. Chem., Int. Ed. 43 (2004) 5530;
(b) M. Tamm, A. Kunst, E. Herdtweck, Chem. Commun. (2005) 1729;
(c) M. Tamm, A. Kunst, T. Bannenberg, S. Randoll, P.G. Jones, Organometallics 26 (2007) 417.
[6] C. Elschenbroich, F. Paganelli, M. Nowotny, B. Neumüller, O. Burghaus, Z. Anorg. Allg. Chem. 630 (2004) 1599.
[7] (a) H. Braunschweig, M. Lutz, K. Radacki, Angew. Chem., Int. Ed. 44 (2005) 5647;
(b) A. Bartole-Scott, H. Braunschweig, T. Kupfer, M. Lutz, I. Manners, T. Nguyen, K. Radacki, F. Seeler, Chem. Eur. J. 12 (2006) 1266;
(c) H. Braunschweig, M. Lutz, K. Radacki, A. Schaumlöffel, F. Seeler, C. Unkelbach, Organometallics 25 (2006) 4433;
(d) H. Braunschweig, T. Kupfer, M. Lutz, K. Radacki, J. Am. Chem. Soc. 129 (2007) 8893.
[8] M. Tamm, A. Kunst, T. Bannenberg, E. Herdtweck, R. Schmid, Organometallics 24 (2005) 3163.
[9] R.J. Baker, T. Bannenberg, A. Kunst, S. Randoll, M. Tamm, Inorg. Chim. Acta 359 (2006) 4797.
[10] G. Menconi, N. Kaltsoyannis, Organometallics 24 (2005) 1189.
[11] (a) J. Blenkers, P. Bruin, J.H. Teuben, J. Organomet. Chem. 291 (1985) 61;
(b) R.R. Andréa, A. Terpstra, A. Oskam, P. Bruin, J.H. Teuben, J. Organomet. Chem 307 (1986) 307;
(c) R.D. Rogers, J.H. Teuben, J. Organomet. Chem. 354 (1988) 169.

[12] (a) M.L.H. Green, N.M. Walker, J. Chem. Soc., Chem. Commun. (1989) 1865;
(b) G.M. Diamond, M.L.H. Green, P. Mountford, N. M Walker, J.A.K. Howard, J. Chem. Soc., Dalton Trans. (1992) 417.

[13] N. Kuhn, T. Kratz, Synthesis (1993) 561.

[14] P.M. Druce, B. M Kingston, M.F. Lappert, T.R. Spalding, R.C. Srivastava, J. Chem. Soc. (A) (1969) 2106.

[15] GAUSSIAN 03, Revision C.02, M.J. Frisch, G.W. Trucks, H.B. Schlegel, G.E. Scuseria, M.A. Robb, J.R. Cheeseman, J.A. Montgomery Jr., T. Vreven, K.N. Kudin, J.C. Burant, J.M. Millam, S.S. Iyengar, J. Tomasi, V. Barone, B. Mennucci, M. Cossi, G. Scalmani, N. Rega, G.A. Petersson, H. Nakatsuji, M. Hada, M. Ehara, K. Toyota, R. Fukuda, J. Hasegawa, M. Ishida, T. Nakajima, Y. Honda, O. Kitao, H. Nakai, M. Klene, X. Li, J.E. Knox, H.P. Hratchian, J.B. Cross, V. Bakken, C. Adamo, J. Jaramillo, R. Gomperts, R.E. Stratmann, O. Yazyev, A.J. Austin, R. Cammi, C. Pomelli, J.W. Ochterski, P.Y. Ayala, K. Morokuma, G.A. Voth, P. Salvador, J.J. Dannenberg, V.G. Zakrzewski, S. Dapprich, A.D. Daniels, M.C. Strain, O. Farkas, D.K. Malick, A.D. Rabuck, K. Raghavachari, J.B. Foresman, J.V. Ortiz, Q. Cui, A.G. Baboul, S. Clifford, J. Cioslowski, B.B. Stefanov, G. Liu, A. Liashenko, P. Piskorz, I. Komaromi, R.L. Martin, D.J. Fox, T. Keith, M.A. Al-Laham, C.Y. Peng, A. Nanayakkara, M. Challacombe, P.M.W. Gill, B. Johnson, W. Chen, M.W. Wong, C. Gonzalez, J.A. Pople, Gaussian, Inc., Wallingford CT, 2004.

[16] (a) A.D. Becke, J. Chem. Phys. 98 (1993) 5648;
(b) C. Lee, W. Yang, R.G. Parr, Phys. Rev. B 37 (1988) 785.

[17] Y. Zhao, N.E. Schultz, D.G. Truhlar, J. Chem. Theory Comput. 2 (2006) 364.

[18] M. Dolg, H. Stoll, H. Preuss, R.M. Pitzer, J. Phys. Chem. 97 (1993) 5852.

[19] G.M. Sheldrick, Acta Cryst. A 64 (2008) 112.

[20] (a) K.A. Lyssenko, M.Y. Antipin, S.Y. Ketkov, Russ. Chem. Bull. Int. Ed. 50 (2001) 130;
(b) J.D. Zeinstra, J.L. de Boer, J. Organomet. Chem. 54 (1973) 207.

[21] R.D. Shannon, Acta Cryst. A32 (1976) 751.

[22] (a) D. Gourier, D. Samuel, Inorg. Chem. 27 (1988) 3018;
(b) A.B.P. Lever, S.I. Gorelsky, Struct. Bond. 107 (2004) 77.

[23] J.C. Green, N. Kaltsoyannis, K.H. Sze, M. MacDonald, J. Am. Chem. Soc. 116 (1994) 1994.

[24] D. Sutton, Electronic Spectra of Transition Metal Complexes, McGraw-Hill, London, 1968.

[25] For [(η⁷-C₇H₇)M(η⁵-C₅Me₅)] the following values have been reported [11a]: M = Ti, λ = 675 nm, ε = 32 L mol⁻¹ cm⁻¹; M = Zr, λ = 535 nm, ε = 160 L mol⁻¹ cm⁻¹; M = Hf, λ = 476 nm, ε = 145 L mol⁻¹ cm⁻¹.

[26] R.W. Stephany, M.J.A. de Bie, W. Drenth, Org. Magn. Reson. 6 (1974) 45. In our hands, 2,6-dimethylphenyl isocyanide shows ν(CN) = 2123 cm⁻¹ in KBr, and a THF solution of tert-butyl isocyanide shows a strong band at 2132 cm⁻¹.

[27] (a) T. Brackemeyer, G. Erker, R. Fröhlich, Organometallics 16 (1997) 531;
(b) W. Ahlers, G. Erker, R. Fröhlich, J. Organomet. Chem. 571 (1998) 83;
(c) W. Ahlers, G. Erker, R. Fröhlich, U. Peuchert, J. Organomet. Chem. 578 (1999) 115.

[28] L.B. Kool, M.D. Rausch, M. Herberhold, H.G. Alt, U. Thewalt, B. Honold, Organometallics 5 (1986) 2465.

[29] P. Berno, C. Floriani, A. Chiesi-Villab, C. Rizzoli, J. Chem. Soc., Dalton Trans. (1991) 3085.

[30] J.E. Bol, B. Hessen, J.H. Teuben, W.J.J. Smeets, A.L. Spek, Organometallics 11 (1992) 1981.

[31] H. Jacobsen, H. Berke, T. Brackemeyer, T. Eisenblätter, G. Erker, R. Fröhlich, O. Meyer, K. Bergander, Helv. Chim. Acta 81 (1998) 1692.

[32] T. Mathieson, A. Schier, H. Schmidbaur, J. Chem. Soc., Dalton Trans. (2001) 1196.

[33] M. Niehues, G. Kehr, G. Erker, B. Wibbeling, R. Frölich, O. Blacque, H. Berke, J. Organomet. Chem. 663 (2002) 192.

[34] M. Niehues, G. Kehr, R. Fröhlich, G. Erker, Z. Naturforsch. 58b (2003) 1005.

[35] M.D. Fryzuk, T.S. Haddad, D.J. Berg, Coord. Chem. Rev. 99 (1990) 137.

[36] (a) The Cambridge Structural Database (CSD version 5.29, November 2007) contains 102 structures of Zr–PMe₃ complexes; the Zr–P distances range from 2.638 to 2.831 Å with a mean value of 2.735 Å (one example featuring a Zr–P distance of 3.033 Å was discarded).;
(b) The Cambridge Structural Database (CSD version 5.29, November 2007) contains 17 structures of Hf–PMe₃ complexes; the distances range from 2.641 to 2.761 Å with a mean value of 2.715 Å.

[37] M.L.H. Green, P. Mountford, N.M. Walker, J. Chem. Soc., Chem. Commun. (1989) 908.

[38] (a) D. Bourissou, O. Guerret, F.P. Gabba, G. Bertrand, Chem. Rev. 100 (2000) 39;
(b) F.E. Hahn, M.C. Jahnke, Angew. Chem. 120 (2008) 3166. Angew. Chem., Int. Ed. 47 (2008) 3122.

[39] (a) S. Grimme, Angew. Chem. 118 (2006) 4571. Angew. Chem., Int. Ed. Engl. 45 (2006) 4460;
(b) Y. Zhao, D.G. Thruhlar, Acc. Chem. Res. 41 (2008) 157.

[40] (a) Y. Zhao, D.G. Truhlar, Org. Lett. 9 (2007) 1967;
(b) S. Torker, D. Merki, P. Chen, J. Am. Chem. Soc. 130 (2008) 4808.

[41] N.M. Scott, H. Clavier, P. Mahjoor, E.D. Stevens, S.P. Nolan, Organometallics 27 (2008) 3181. and references cited therein.

[42] (a) S. Díez-González, S.P. Nolan, Coord. Chem. Rev. 251 (2007) 874;
(b) L. Jafarpour, S.P. Nolan, Adv. Organomet. Chem. 46 (2001) 181.

[43] P.B. Dias, M.E. Minas de Piedade, J.A. Martinho Simões, Coord. Chem. Rev. 135/136 (1994) 737.

[44] (a) S.K. Ritter, Chem. Eng. News 85 (41) (2007) 42;
(b) C. Marschner, Angew. Chem., Int. Ed. 46 (2007) 6770;
(c) Y. Okhi, M.D. Fryzuk, Angew. Chem., Int. Ed. 46 (2007) 3180.

[45] (a) Selected examples: T. Beweries, V.V. Burlakov, M.A. Bach, S. Peitz, P. Arndt, W. Baumann, A. Spannenberg, U. Rosenthal, B. Pathak, E.D. Jemmis, Angew. Chem., Int. Ed. 46 (2007) 6907;
(b) W.H. Bernskoetter, E. Lobkovsky, P.J. Chirik, Angew. Chem., Int. Ed. 46 (2007) 2858;
(c) T. Beweries, V.V. Burlakov, M.A. Bach, P. Arndt, W. Baumann, A. Spannenberg, U. Rosenthal, Organometallics 26 (2007) 247.